Optimal Donor Selection Across Multiple Outcomes For Hematopoietic Stem Cell Transplantation By Bayesian Nonparametric Machine Learning

Rodney A Sparapani[1], Martin Maiers[2], Stephen R. Spellman[2], Bronwen E Shaw[3], Purushottam W Laud[1], Steven M. Devine[2], and Brent R Logan[1]

[1]Division of Biostatistics, Medical College of Wisconsin, Milwaukee, WI, USA
[2]CIBMTR (Center for International Blood and Marrow Transplant Research), NMDP, Minneapolis, MN, USA
[3]CIBMTR, Department of Medicine, Medical College of Wisconsin, Milwaukee, WI, USA

May 9, 2024

Abstract

Allogeneic hematopoietic cell transplantation (HCT) is one of the only curative treatment options for patients suffering from life-threatening hematologic malignancies; yet, the possible adverse complications can be serious even fatal. Matching between donor and recipient for 4 of the HLA genes is widely accepted and supported by the literature. However, among 8/8 allele matched unrelated donors, there is less agreement among centers and transplant physicians about how to prioritize donor characteristics like additional HLA loci (DPB1 and DQB1), donor sex/parity, CMV status, and age to optimize transplant outcomes. This leads to varying donor selection practice from patient to patient or via center protocols. Furthermore, different donor characteristics may impact different post transplant outcomes beyond mortality, including disease relapse, graft failure/rejection, and chronic graft-versus-host disease (components of event-free survival, EFS). We develop a general methodology to identify optimal treatment decisions by considering the trade-offs on multiple outcomes modeled using Bayesian nonparametric machine learning. We apply the proposed approach to the problem of donor selection to optimize overall survival and event-free survival, using a large outcomes registry of HCT recipients and their actual and potential donors from the Center for

International Blood and Marrow Transplant Research (CIBMTR). Our approach leads to a donor selection strategy that favors the youngest male donor, except when there is a female donor that is substantially younger.

1 Introduction

The discovery of stem cells in 1963 [McCulloch and Till, 2005] has lead to new avenues of treatment for a variety of illnesses including blood-borne cancers, auto-immune diseases and inherited newborn conditions. Allogeneic hematopoietic cell transplantation (HCT) is the only curative treatment option for patients suffering from life-threatening hematologic malignancies; yet, the possible adverse complications can be serious even fatal. Stem cells are harvested from a donor that is HLA matched to the transplant recipient. In 2021 for the United States (US) alone, 9,349 allogeneic HSCT treatments were performed [Center for International Blood and Marrow Transplant Research, 2024] and unrelated volunteers donated their stem cells for 5,073 (54%) of those (the remainder of donors were kin). The National Marrow Donor Program (NMDP) in the US maintains the world's largest stem cell registry of more than 9 million donors and potential donors, and facilitates access to more then 42 million donors worldwide through the World Marrow Donor Association. For patients without an HLA-matched family member, a donor search is conducted by the NMDP registry. HLA matching is critical to preventing/mitigating graft vs. host disease (GVHD) by ensuring antigen cross-compatibility with the transplanted immune system. However, all matched unrelated donors (MUD) do not necessarily have the same prognostic risks/benefits. Besides HLA loci, other donor characteristics are considered including age, sex/child-bearing parity, cytomegalovirus (CMV) serostatus. Previous research has consistently found survival benefits associated with choosing a younger MUD [Kollman et al., 2001, 2016, Shaw et al., 2018, Pidala et al., 2019, Logan et al., 2021]. But, the optimization potential for selection of other donor factors has not been consistently shown [Shaw et al., 2007, Fleischhauer et al., 2012, Pidala et al., 2014, Fleischhauer et al., 2017, Shaw et al., 2017]. Therefore, donor selection practices vary from patient to patient (or via center to center protocols), providing us with the opportunity to utilize modern machine learning techniques to determine which factors will yield the best possible outcomes.

Several complications arise in optimizing donor selection. First, donor selection requires consideration of multiple donor factors from a finite but sometimes large list of potential MUDs specific to a given recipient. Therefore, practical implementation of optimal donor selection requires a good understanding of what donor characteristics are necessary to be considered in an optimization algorithm. Second, donor selection should be individualized, since the impact of donor factors may be dependent on patient or disease characteristics; this necessitates that a prediction model for patient outcomes has sufficient flexibility to capture complex interactions. Third, selecting an optimal donor depends on what outcome is being optimized. Overall survival is of greatest importance,

but there are other post-transplant complications such as clinical relapse, graft failure and/or GVHD causing severe morbidity that could be impacted by donor characteristics.

We develop optimal donor selection methodology as an individualized decision for a potential recipient while considering multiple outcomes along with the likely trade-offs amongst them. Prior to optimization, we examine the impact of various donor characteristics on relevant outcomes: narrowing to a relatively parsimonious subset for the implementation of the donor search. Next, we develop an optimal donor selection method with multiple outcomes. Qian and Murphy [2011] show that the optimal individualized treatment rule assigns each patient to the treatment with the optimal conditional expectation given their patient characteristics. Following this, we propose to optimize donor selection by directly selecting the donor whose characteristics optimize the expected outcome for a given patient based on a prediction model. Furthermore, accurate predictive modeling is sufficient to identify an optimal treatment rule [Qian and Murphy, 2011]. From training data, we construct prediction models for overall survival (OS) and event-free survival (EFS is a composite of death, clinical relapse, graft failure/rejection or moderate/severe chronic GVHD) with a nonparametric machine learning framework based on Bayesian Additive Regression Trees (BART) Chipman et al. [2010]. BART models have three key features which make them useful in this setting: 1) excellent predictive performance; 2) automatically incorporate complex interactions; and 3) avoiding precarious restrictive assumptions like linearity. On a solid foundation of Bayesian inference, BART inherently provides uncertainty quantification of any model predictions as well as any function of them. The development of BART models for survival outcomes has demonstrated increasing flexibility [Bonato et al., 2011, Sparapani et al., 2016, Henderson et al., 2020, Linero et al., 2022, Sparapani et al., 2023]. We will employ Nonparametric Failure Time BART (NFT BART) [Sparapani et al., 2023] for predictive modeling that avoids restrictive assumptions (such as proportionality, homoskedasticity and normality) while providing computational scalability to large data sets like we have here. After predictive modeling is performed for each outcome, we create a weighted utility from the OS and EFS expectations from each potential donor to a given recipient. Now, we select the donor which optimizes the weighted utility function. Weights represent the desired relative importance of the outcomes. We demonstrate several optimal donor selection policies via different weights.

2 Methods

2.1 Data Sources

Clinical outcome data was obtained from the Center for International Blood and Marrow Transplant Research (CIBMTR) research database. CIBMTR is a research collaboration between the NMDP and the Medical College of Wisconsin which collects outcome data for all allogeneic HSCT recipients in the

US as the custodian of the Stem Cell Therapeutic Outcomes Database under the C.W. Bill Young Transplantation Program of the Health Resources and Services Administration [Stem Cell Therapeutic and Research Act Reauthorization, 2021]. Our cohort consisted of all HCT recipients in the US from 2016 to 2019 with 8/8 high-resolution matching at HLA-A, B, C, and DRB1 to their unrelated donor. All patients provided informed consent for participation in the CIBMTR Research Database and the study was approved by the NMDP Institutional Review Board. We randomly divided our cohort into a subset of 10,016 patients (85%) for training prediction models and 1,802 (15%) for validation of the prediction models. Within the validation subset, 699 (39%) had their search archive records available. The NMDP search archive database is a snapshot of each patient's donor search prior to transplant that includes all of the potentially matched unrelated donors on the registry at the time of the search. This allows us to re-conduct the donor search using our proposed donor selection algorithms and assess how the proposed strategies will perform in practice, compared to the real-world donor selection practice based on the actual donor selected. Since we typically do not know the high-resolution HLA typing and match status of all potential donors at the time of the search, we restrict the donor list for each patient in the search archive subset to likely 8/8 matches (for volunteers whose HLA typing is ambiguous [Paunić et al., 2016], we only consider those matches with a probability ≥ 0.9 based on HapLogic predictions [Dehn et al., 2016]). The additional donor characteristics beyond the requisite 8/8 HLA matching to be considered for optimal selection are age, sex/child-bearing parity, CMV status, HLA -DPB1 and/or -DQB1.

2.2 Study Endpoints

We focus on optimizing both overall survival/mortality (OS) and event-free survival (EFS) that is defined as a composite of death, clinical relapse, graft failure/rejection, moderate/severe chronic GVHD: whichever comes first. Since transplant is a curative therapy with OS/EFS curves flattening substantially by 3 years, we focus on this time horizon by optimizing OS/EFS by either the point-wise 3 year probabilities, or the restricted mean survival time (RMST) up to 3 years. RMST is an alternative framing of survival outcomes that may have advantages over point-wise analysis or proportional hazards modeling, particularly in interpretation [Royston and Parmar, 2013, Pak et al., 2017, Kloecker et al., 2020].

2.3 Statistical Analysis

We fit NFT BART prediction models to the OS and EFS data using the **nftbart** R package [Sparapani et al., 2023]. Posterior samples of survival predictions are generated for a patient p with characteristics x_p who is a recipient of transplantation from donor d with characteristics z_d, given by $S_m(t|x_p, z_d, \mathcal{D})$, for draws $m = 1, \ldots, M$. Here we use $\mathcal{D}$ in this Bayesian model to represent that inference in the model is conditional on the observed data, including the

event/censoring times, event indicators, and measured covariates. Similarly, we generate posterior samples of predictions for RSMT up to time t, defined by $\text{RMST}_m(t|x_p, z_d, \mathcal{D}) \equiv \int_0^t S_m(s|x_p, z_d, \mathcal{D})\text{d}s$ (see Section 6 of the Supplement for more details on these calculations). We use the posterior mean of these samples to summarize predictions and to perform optimizations; in particular, $E[S(t|x_p, z_d, \mathcal{D})] \approx M^{-1}\sum_m S_m(t|x_p, z_d, \mathcal{D})$ and $E[\text{RMST}(t|x_p, z_d, \mathcal{D})] \approx M^{-1}\sum_m \text{RMST}_m(t|x_p, z_d, \mathcal{D})$. Furthermore, the posterior samples can be used to quantify uncertainty, e.g., the $(1-q)\times 100\%$ credible interval for survival is $S_m(t|x_p, z_d, \mathcal{D}) : S_{m'}(t|x_p, z_d, \mathcal{D})$ where m (m') is the $q/2 \times 100\%$ ($1 - q/2 \times 100\%$) posterior quantile. Waterfall plots [Gillespie, 2012] were generated to describe changes in predicted outcomes for each patient as an individual donor characteristic was varied one at a time while holding the others fixed. For example, the waterfall plot for donor sex in the bottom row of Figure 1 shows the predictions (posterior means) for each transplant if the donor had been male vs. female. Waterfall plots showing little to no impact in survival for all, or nearly all, patients attributable to a donor characteristic change indicate a negligible impact that can be simply ignored. We define a negligible difference of < 1 % in predicted survival at 3 years or < 10 days in RMST as an indifference zone [Soeteman et al., 2020]. After this donor characteristic selection was completed the NFT BART model was refitted with the relevant donor characteristics for further evaluation on donor optimization. Note that prediction models are built for both OS and EFS. Notationally, we refer to the posterior mean OS or EFS as $E[\text{OS}(t|x_p, z_d, \mathcal{D}]$ and $E[\text{EFS}(t|x_p, z_d, \mathcal{D}]$ respectively; and to posterior mean RMST OS or EFS as $E[\text{RMOS}(t|x_p, z_d, \mathcal{D})]$ and $E[\text{RMEFS}(t|x_p, z_d, \mathcal{D})]$ respectively.

To optimize donor selection, we follow the approach of Qian and Murphy [2011] who show that an optimal individualized treatment rule assigns each patient to the treatment which has the best conditional expectation given their patient characteristics. Here we define an optimal donor selection rule by selecting the donor which has the best expected outcome from our NFT BART prediction model according to the selected donor features. To address multiple outcomes of OS and EFS, we optimize a utility function which is a weighted average of the OS and EFS outcomes. The weight parameter represents the relative importance of the corresponding outcome in terms of the donor selection rule. The optimal donor for patient p among their set D_p of potential donors is defined as

$$d_p^{\text{opt}} \equiv \arg\max_{d \in D_p} \{wE[\text{OS}(t|x_p, z_d, \mathcal{D})] + (1-w)E[\text{EFS}(t|x_p, z_d, \mathcal{D})]\}$$

for the pointwise survival probability outcome (and similarly defined for RMST). Note that a weight of $w = 1$ represents donor optimization based solely on OS as opposed to $w = 0$ for EFS only. Weights between $0.5 < w < 1$ tend to have greater emphasis on optimizing OS, yet still improving EFS particularly in situations where OS differences are small. The posterior mean OS and EFS probabilities for this optimal donor are $E[\text{OS}(t|x_p, z_{d_p^{\text{opt}}}, \mathcal{D})]$ and $E[\text{EFS}(t|x_p, z_{d_p^{\text{opt}}}, \mathcal{D})]$ respectively.

We benchmark the optimal donor strategy performance against the actual donor d_p^{actual} used for each transplant in the search archive by taking the difference in posterior mean OS or EFS, according to the following.

$$\text{OS}_p^{\text{diff}}(t) \equiv E[\text{OS}(t|x_p, z_{d_p^{\text{opt}}}, \mathcal{D})] - E[\text{OS}(t|x_p, z_{d_p^{\text{actual}}}, \mathcal{D})]$$
$$\text{EFS}_p^{\text{diff}}(t) \equiv E[\text{EFS}(t|x_p, z_{d_p^{\text{opt}}}, \mathcal{D})] - E[\text{EFS}(t|x_p, z_{d_p^{\text{actual}}}, \mathcal{D})]$$

Plots of $\text{OS}_p^{\text{diff}}(t)$ vs. $\text{EFS}_p^{\text{diff}}(t)$ by patient for different values of w are constructed to show how w impacts the tradeoffs between the two outcomes.

The population level outcome for an optimal donor strategy is obtained by averaging the optimal outcomes across a sample of patients as follows.

$$\text{OS}^{\text{opt}}(t) \equiv E_p\{E[\text{OS}(t|x_p, z_{d_p^{\text{opt}}}, \mathcal{D}]\}$$
$$\text{EFS}^{\text{opt}}(t) \equiv E_p\{E[\text{EFS}(t|x_p, z_{d_p^{\text{opt}}}, \mathcal{D}]\}$$

Population level outcomes for the actual donor strategy can be similarly defined, as well as differences in population level outcomes between the optimal and actual donor strategy. Note also that posterior samples of the population level outcomes can be obtained by applying the optimization on a posterior sample basis. Finally, we have shown an optimal donor selection rule based on the weighted average of the OS and EFS probabilities at time t. An optimal donor selection rule based on a weighted average of the RMST for OS and EFS up to time t could be similarly derived.

3 Results

Among the recipients within the training (validation) set, 37.3% (38.4%) died whereas among the censored survivors the median days of follow-up was 749 (745) with a first:third quartile of 391:1117 (390:1110). Similarly, for EFS, 61.3% (61.6%) suffered the event with median survivor days of follow-up of 741 (737) and first:third quartile 383:1107 (382:1100) for training (validation) respectively. We summarize the collected data in a series of tables for recipients, donors and disease characteristics: the **bold** variables are included in the model (additional model variables that are not shown here appear in the Supplement Tables 2 through 6). The cohort of recipients consists mainly of those 40 or older: about three-quarters (74.1%); see Table 1. The donors are comparatively younger: 88.5% are below 40; see Table 2. Almost three-quarters of the patients, 73%, were stricken by the three most common hematologic cancers: acute lymphoblastic leukemia (ALL), 13%; acute myeloid leukemia (AML), 40%; and myelodysplastic syndrome (MDS), 20%; see Table 3.

Now we turn to the decision-making process for which donor characteristics will optimize recipient outcomes. In Supplement Table 7, you will find a list of waterfall plots representing donor choices with respect to age, sex/parity, CMV, DPB1 and DQB1. First, we eliminate those factors that are not promising. Matching based on the criteria of CMV and DPB1 was not productive for either

OS or EFS: in all cases, the expected benefit is within the indifference zone; see Supplement Figures 12, 14, 16 and 18. With respect to DQB1, we can see that matching is already being undertaken at a high rate (Table 2): only 4.4% are mismatched when available. Therefore, it is possible that we did not have sufficient data to investigate matching of DQB1 due to the relatively few mismatches; waterfall plots are provided by Supplement Figures 20 and 22. Waterfall plots for parity (parous vs. non-parous females) show that the difference between these donors is negligible; see Supplement Figures 7 to 10.

This leaves us with just age and sex. So, we refit the models narrowing the donor characteristics to age and sex for optimization predicting OS and EFS outcomes for each patient in the validation set. The plot for age shows that choosing a younger donor is beneficial for OS and to a lesser extent EFS: generally, a donor aged 30 or less is preferable with marginal gains achieved going further than that; see the upper half of Figure 1. For OS, the choice of sex (male vs. female) is indifferent as seen in the bottom right of Figure 1. But, on the contrary for EFS, the choice of sex is quite important: males are generally preferable to females, with the effect of sex being larger than the donor age effect for EFS; see the bottom left of Figure 1. Putting this together for both age and sex across both EFS and OS endpoints, we see that the youngest male is generally preferable due to EFS benefit except when a much younger female is available. In the latter case the OS benefit from younger age may be more clinically important than an EFS benefit from the male donor. As we might expect, this story is largely the same if we are considering differences in RMST rather than survival probabilities; see Figure 2. In Figure 3, we see scatter-plots for OS(3) vs. EFS(3) differentials with three donor choice strategies. Also shown in the figure is the number of female and male donors selected outside and inside the indifference zone. Optimizing OS(3) favors the youngest female (355 females and 103 males outside the indifference zone). Optimizing EFS(3) favors the youngest male (2 females and 280 males outside the indifference zone). Finally, optimizing 2OS(3):1EFS(3) generally favors the youngest male except when there is a considerably younger female available (35 females and 253 males outside the indifference zone). In Figure 4, we plot the population-level value function with respect to these donor choice strategies; optimizing 2OS(3):1EFS(3) provides near-optimal performance for OS(3) and EFS(3) differentials respectively.

4 Conclusions

In this article, we proposed a novel approach to optimize treatment across multiple outcome variables, using a weighted utility function, to prioritize treatments having the best results for the most important clinical outcomes. We used a flexible machine learning approach for survival data called NFT BART to build prediction models. This model makes minimal assumptions, while automatically handling complex relationships with non-linearity and interactions, allowing for patient specific predictions of survival probabilities, or restricted mean survival

times, for different treatment choices. Flexibility to generate patient specific predictions are important in this setting to allow for personalized treatment selection. As a Bayesian approach, NFT BART offers posterior uncertainty summaries for the prediction inference, a benefit that may not be available with other machine learning approaches. We applied the proposed approach to the problem of optimal donor selection for a MUD HCT. Our approach can be readily extended to a general setting with a large number of patient specific treatment options. In the donor selection application patients have different sets of potential donors due to their different HLA typing, and some patients may have a very long list of potential donors to choose from. The main clinical conclusions of this study are that the youngest available male donor should generally be prioritized for all patients, except when there is a female donor considerably younger who would likely have better overall survival outcomes despite lower event-free survival. No other donor factors were important for either overall survival or event-free survival, acknowledging that there was lesser power for determining the impact of HLA-DQB1 due to limited numbers of mismatches on this locus. Although some patients may have many donors to choose from, the monotone effect of donor age and the reduced set of important donor characteristics simplified the optimal donor choice to just selecting between two donors (youngest male and youngest female). However, in general the framework that we used can be implemented even when the decision process does not simplify like this.

There are some limitations to this study. Our study focused on MUD transplants only, and the cohort had limited use of post-transplant cyclophosphamide (PTCy) as a GVHD prophylaxis strategy. PTCy is surging in popularity due to its successful use in matched and mismatched donor transplants. The main benefit of PTCy is in reduced acute and chronic GVHD leading to improvements in EFS, but with limited impact on OS. Future studies using our general strategy should expand to include mismatched donor transplants and consider the impact of PTCy in donor selection strategies. Additionally, there may be other donor factors to be considered in a selection algorithm; as data on these become available, their contribution to donor selection algorithms could be examined using our approach. Finally, we have focused here on an approach of weighting hierarchically ordered survival outcomes for optimization. Future work could investigate a multi-state prediction model with utilities for each state. This would help our understanding of the contribution of different donor characteristics to each of the components for the EFS endpoint.

Acknowledgments

CIBMTR is supported primarily by the Public Health Service U24CA076518 from the National Cancer Institute (NCI), the National Heart, Lung and Blood Institute (NHLBI), and the National Institute of Allergy and Infectious Diseases (NIAID); 75R60222C00011 from the Health Resources and Services Administration (HRSA); and N00014-23-1-2057 and N00014-24-1-2057 from the

Office of Naval Research. Support is also provided by the Medical College of Wisconsin, NMDP, Gateway for Cancer Research, Pediatric Transplantation and Cellular Therapy Consortium and from the following commercial entities: AbbVie; Actinium Pharmaceuticals, Inc.; Adaptive Biotechnologies Corporation; ADC Therapeutics; Adienne SA; Alexion; AlloVir, Inc.; Amgen, Inc.; Astellas Pharma US; AstraZeneca; Atara Biotherapeutics; BeiGene; BioLineRX; Blue Spark Technologies; bluebird bio, inc.; Blueprint Medicines; Bristol Myers Squibb Co.; CareDx Inc.; CSL Behring; CytoSen Therapeutics, Inc.; DKMS; Elevance Health; Eurofins Viracor, DBA Eurofins Transplant Diagnostics; Gamida-Cell, Ltd.; Gift of Life Biologics; Gift of Life Marrow Registry; GlaxoSmithKline; HistoGenetics; Incyte Corporation; Iovance; Janssen Research & Development, LLC; Janssen/Johnson & Johnson; Jasper Therapeutics; Jazz Pharmaceuticals, Inc.; Karius; Kashi Clinical Laboratories; Kiadis Pharma; Kite, a Gilead Company; Kyowa Kirin; Labcorp; Legend Biotech; Mallinckrodt Pharmaceuticals; Med Learning Group; Medac GmbH; Merck & Co.; Mesoblast; Millennium, the Takeda Oncology Co.; Miller Pharmacal Group, Inc.; Miltenyi Biotec, Inc.; MorphoSys; MSA-EDITLife; Neovii Pharmaceuticals AG; Novartis Pharmaceuticals Corporation; Omeros Corporation; OptumHealth; Orca Biosystems, Inc.; OriGen BioMedical; Ossium Health, Inc.; Pfizer, Inc.; Pharmacyclics, LLC, An AbbVie Company; PPD Development, LP; REGiMMUNE; Registry Partners; Rigel Pharmaceuticals; Sanofi; Sarah Cannon; Seagen Inc.; Sobi, Inc.; Stemcell Technologies; Stemline Technologies; STEMSOFT; Takeda Pharmaceuticals; Talaris Therapeutics; Vertex Pharmaceuticals; Vor Biopharma Inc.; Xenikos BV. The views expressed in this article do not reflect the official policy or position of the National Institute of Health, the Department of the Navy, the Department of Defense, Health Resources and Services Administration (HRSA) or any other agency of the U.S. Government.

Data Accessibility Statement

CIBMTR supports accessibility of research in accord with the National Institutes of Health (NIH) Data Sharing Policy and the National Cancer Institute (NCI) Cancer Moonshot Public Access and Data Sharing Policy. The CIBMTR only releases de-identified datasets that comply with all relevant global regulations regarding privacy and confidentiality.

References

V. Bonato, V. Baladandayuthapani, B. M. Broom, E. P. Sulman, K. D. Aldape, and K. A. Do. Bayesian ensemble methods for survival prediction in gene expression data. *Bioinformatics (Oxford, England)*, 27(3):359–367, 2011.

Center for International Blood and Marrow Transplant Research. Summary slides and reports. [https://cibmtr.org/CIBMTR/Resources/Summary-Slides-Reports], 2024.

Hugh A. Chipman, Edward I. George, and Robert E. McCulloch. BART: Bayesian Additive Regression Trees. *The Annals of Applied Statistics*, 4(1): 266–298, 2010.

Jason Dehn, Michelle Setterholm, Kelly Buck, Jane Kempenich, Beth Beduhn, Loren Gragert, Abeer Madbouly, Stephanie Fingerson, and Martin Maiers. HapLogic: a predictive human leukocyte antigen–matching algorithm to enhance rapid identification of the optimal unrelated hematopoietic stem cell sources for transplantation. *Biology of Blood and Marrow Transplantation*, 22(11):2038–2046, 2016.

Katharina Fleischhauer, Bronwen E Shaw, Theodore Gooley, Mari Malkki, Peter Bardy, Jean-Denis Bignon, Valérie Dubois, Mary M Horowitz, J Alejandro Madrigal, Yasuo Morishima, et al. Effect of T-cell-epitope matching at HLA-DPB1 in recipients of unrelated-donor haemopoietic-cell transplantation: a retrospective study. *The lancet oncology*, 13(4):366–374, 2012.

Katharina Fleischhauer, Kwang Woo Ahn, Hai-Lin Wang, Laura Zito, Pietro Crivello, Carlheinz Müller, Michael Verneris, Bronwen E Shaw, Joseph Pidala, Machteld Oudshorn, et al. Directionality of non-permissive HLA-DPB1 T-cell epitope group mismatches does not improve clinical risk stratification in 8/8 matched unrelated donor hematopoietic cell transplantation. *Bone marrow transplantation*, 52(9):1280–1287, 2017.

Theresa W Gillespie. Understanding waterfall plots. *Journal of the advanced practitioner in oncology*, 3(2):106, 2012.

Nicholas C Henderson, Thomas A Louis, Gary L Rosner, and Ravi Varadhan. Individualized treatment effects with censored data via fully nonparametric Bayesian accelerated failure time models. *Biostatistics*, 21(1):50–68, 2020.

David A Karnofsky, Walter H Abelmann, Lloyd F Craver, and Joseph H Burchenal. The use of the nitrogen mustards in the palliative treatment of carcinoma: With particular reference to bronchogenic carcinoma. *Cancer*, 1948.

David E Kloecker, Melanie J Davies, Kamlesh Khunti, and Francesco Zaccardi. Uses and limitations of the restricted mean survival time: illustrative examples from cardiovascular outcomes and mortality trials in Type 2 diabetes. *Annals of internal medicine*, 172(8):541–552, 2020.

Craig Kollman, Craig WS Howe, Claudio Anasetti, Joseph H Antin, Stella M Davies, Alexandra H Filipovich, Janet Hegland, Naynesh Kamani, Nancy A Kernan, Roberta King, et al. Donor characteristics as risk factors in recipients after transplantation of bone marrow from unrelated donors: the effect of donor age. *Blood, The Journal of the American Society of Hematology*, 98(7): 2043–2051, 2001.

Craig Kollman, Stephen R Spellman, Mei-Jie Zhang, Anna Hassebroek, Claudio Anasetti, Joseph H Antin, Richard E Champlin, Dennis L Confer, John F DiPersio, Marcelo Fernandez-Viña, et al. The effect of donor characteristics on survival after unrelated donor transplantation for hematologic malignancy. *Blood, The Journal of the American Society of Hematology*, 127(2):260–267, 2016.

Antonio R Linero, Piyali Basak, Yinpu Li, and Debajyoti Sinha. Bayesian survival tree ensembles with submodel shrinkage. *Bayesian Analysis*, 17(3): 997–1020, 2022.

Brent R Logan, Martin J Maiers, Rodney A Sparapani, Purushottam W Laud, Stephen R Spellman, Robert E McCulloch, and Bronwen E Shaw. Optimal donor selection for hematopoietic cell transplantation using Bayesian machine learning. *JCO clinical cancer informatics*, 5:494–507, 2021.

Ernest A McCulloch and James E Till. Perspectives on the properties of stem cells. *Nature Medicine*, 11(10):1026–1028, 2005.

Kyongsun Pak, Hajime Uno, Dae Hyun Kim, Lu Tian, Robert C Kane, Masahiro Takeuchi, Haoda Fu, Brian Claggett, and Lee-Jen Wei. Interpretability of cancer clinical trial results using restricted mean survival time as an alternative to the hazard ratio. *JAMA oncology*, 3(12):1692–1696, 2017.

Vanja Paunić, Loren Gragert, Joel Schneider, Carlheinz Müller, and Martin Maiers. Charting improvements in US registry HLA typing ambiguity using a typing resolution score. *Human immunology*, 77(7):542–549, 2016.

J. Pidala, S. J. Lee, K. W. Ahn, S. Spellman, H. L. Wang, M. Aljurf, M. Askar, J. Dehn, M. Fernandez Vina, A. Gratwohl, V. Gupta, R. Hanna, M. M. Horowitz, C. K. Hurley, Y. Inamoto, A. A. Kassim, T. Nishihori, and Mueller. Nonpermissive HLA-DPB1 mismatch increases mortality after myeloablative unrelated allogeneic hematopoietic cell transplantation. *Blood*, 124(16):2596–2606, 2014.

Joseph Pidala, Tatenda G Mupfudze, Tammy Payton, Juliet Barker, Miguel-Angel Perales, Bronwen E Shaw, Marcelo Fernández-Viña, Linda J Burns, and Jason Dehn. Urgent time to allogeneic hematopoietic cell transplantation: a national survey of transplant physicians and unrelated donor search coordinators facilitated by the histocompatibility advisory group to the National Marrow Donor Program. *Biology of Blood and Marrow Transplantation*, 25 (12):2501–2506, 2019.

M. Qian and S. A. Murphy. Performance guarantees for individualized treatment rules. *Annals of statistics*, 39(2):1180–1210, 2011.

Patrick Royston and Mahesh KB Parmar. Restricted mean survival time: an alternative to the hazard ratio for the design and analysis of randomized trials with a time-to-event outcome. *BMC medical research methodology*, 13:1–15, 2013.

Bronwen E Shaw, Theodore A Gooley, Mari Malkki, J Alejandro Madrigal, Ann B Begovich, Mary M Horowitz, Alois Gratwohl, Olle Ringdén, Steven GE Marsh, and Effie W Petersdorf. The importance of HLA-DPB1 in unrelated donor hematopoietic cell transplantation. *Blood, The Journal of the American Society of Hematology*, 110(13):4560–4566, 2007.

Bronwen E Shaw, Neema P Mayor, Richard M Szydlo, WP Bultitude, C Anthias, K Kirkland, J Perry, A Clark, S Mackinnon, DI Marks, et al. Recipient/donor HLA and CMV matching in recipients of T-cell-depleted unrelated donor haematopoietic cell transplants. *Bone marrow transplantation*, 52(5): 717–725, 2017.

Bronwen E Shaw, Brent R Logan, Stephen R Spellman, Steven GE Marsh, James Robinson, Joseph Pidala, Carolyn Hurley, Juliet Barker, Martin Maiers, Jason Dehn, et al. Development of an unrelated donor selection score predictive of survival after HCT: donor age matters most. *Biology of Blood and Marrow Transplantation*, 24(5):1049–1056, 2018.

Djøra I Soeteman, Stephen C Resch, Hawre Jalal, Caitlin M Dugdale, Martina Penazzato, Milton C Weinstein, Andrew Phillips, Taige Hou, Elaine J Abrams, Lorna Dunning, et al. Developing and validating metamodels of a microsimulation model of infant HIV testing and screening strategies used in a decision support tool for health policy makers. *MDM Policy & Practice*, 5 (1):1–11, 2020.

Mohamed L Sorror, Brent R Logan, Xiaochun Zhu, J Douglas Rizzo, Kenneth R Cooke, Philip L McCarthy, et al. Prospective validation of the predictive power of the hematopoietic cell transplantation comorbidity index: a Center for International Blood and Marrow Transplant Research study. *Biology of Blood and Marrow Transplantation*, 21(8):1479–1487, 2015.

R. A. Sparapani, B. R. Logan, R. E. McCulloch, and P. W. Laud. Nonparametric survival analysis using Bayesian Additive Regression Trees (BART). *Statistics in medicine*, 35:2741–2753, 2016.

Rodney A Sparapani, Brent R Logan, Martin J Maiers, Purushottam W Laud, and Robert E McCulloch. Nonparametric failure time: Time-to-event machine learning with heteroskedastic Bayesian additive regression trees and low information omnibus Dirichlet process mixtures. *Biometrics*, 79:3023–3037, 2023. [https://cran.r-project.org/package=nftbart].

Stem Cell Therapeutic and Research Act Reauthorization, 2021. [https://bloodstemcell.hrsa.gov].

Elisabetta Zino, Guido Frumento, Sarah Marktel, Maria Pia Sormani, Francesca Ficara, Simona Di Terlizzi, Anna Maria Parodi, Ruhena Sergeant, Miryam Martinetti, Andrea Bontadini, et al. A T-cell epitope encoded by a subset of HLA-DPB1 alleles determines nonpermissive mismatches for hematologic stem cell transplantation. *Blood*, 103(4):1417–1424, 2004.

Table 1: Recipient demographic characteristics. Training and validation sets are mutually exclusive while search archive is a subset of validation. Within the total rows, we present Pearson's Chi-squared test p-values for the comparisons between training with validation and training with search archive: missing values excluded. **Bold** variables are included in the model.

	Training set		Validation set		Search archive		Overall total	
Recipient age	10016		1802	0.0107	699	0.2030	11818	
0:19	1159	11.6%	179	9.9%	73	10.4%	1338	11.3%
20:39	1470	14.7%	255	14.2%	112	16.0%	1725	14.6%
40:59	3167	31.6%	537	29.8%	200	28.6%	3704	31.3%
60:82	4220	42.1%	831	46.1%	314	44.9%	5051	42.7%
Recipient sex	10016		1802	0.6451	699	0.6712	11818	
F	4188	41.8%	743	41.2%	298	42.6%	4931	41.7%
Race	9667		1745	0.7780	675	0.3677	11412	
White	8993	93.0%	1619	92.8%	636	94.2%	10612	93.0%
Black	307	3.2%	57	3.3%	17	2.5%	364	3.2%
Asian	281	2.9%	56	3.2%	15	2.2%	337	3.0%
Other	86	0.9%	13	0.7%	7	1.0%	99	0.9%
Missing	349		57		24		406	
Hispanic ethnicity	9657		1721	0.5746	669	0.7742	11378	
Yes	764	7.9%	143	8.3%	55	8.2%	907	8.0%
Missing	359		81		30		440	
HCT-CI	9932		1785	0.0608	694	0.5969	11717	
0	2093	21.1%	333	18.7%	135	19.5%	2426	20.7%
1:3	4736	47.7%	868	48.6%	337	48.6%	5604	47.8%
4+	3103	31.2%	584	32.7%	222	32.0%	3687	31.5%
Missing	84		17		5		101	
KPS	9807		1764	0.3545	688	0.2613	11571	
10:70	1412	14.4%	247	14.0%	100	14.5%	1659	14.3%
80	2896	29.5%	557	31.6%	226	32.8%	3453	29.8%
90	3971	40.5%	701	39.7%	257	37.4%	4672	40.4%
100	1528	15.6%	259	14.7%	105	15.3%	1787	15.4%
Missing	209		38		11		247	
Median income (ZCTA)	9813		1751	0.7223	679	0.0016	11564	
<25000	33	0.3%	5	0.3%	4	0.6%	38	0.3%
25000, <50000	2619	26.7%	471	26.9%	210	30.9%	3090	26.7%
50000, <75000	3910	39.8%	707	40.4%	279	41.1%	4617	39.9%
75000, <125000	2858	29.1%	510	29.1%	175	25.8%	3368	29.1%
125000+	393	4.0%	58	3.3%	11	1.6%	451	3.9%
Missing	203		51		20		254	

F: female, HCT-CI: hematopoietic cell transplant comorbidity index [Sorror et al., 2015],
KPS: Karnofsky perfomance score [Karnofsky et al., 1948], ZCTA: ZIP code tabulation area

Table 2: Donor matching characteristics. Training and validation sets are mutually exclusive while search archive is a subset of validation. Within the total rows, we present Pearson's Chi-squared test p-values for the comparisons between training with validation and training with search archive: missing values excluded. **Bold** variables are included in the model.

	Training set		Validation set		Search archive		Overall total	
Donor age	9941		1791	0.9524	698	0.3400	11732	
17:29	6499	65.4%	1176	65.7%	479	68.6%	7675	65.4%
30:39	2291	23.0%	411	22.9%	146	20.9%	2702	23.0%
40:49	855	8.6%	148	8.3%	52	7.4%	1003	8.5%
50:60	296	3.0%	56	3.1%	21	3.0%	352	3.0%
Missing	75		11		1		86	
Donor sex	9957		1794	0.5212	698	0.0059	11751	
M	6985	70.2%	1245	69.4%	524	75.1%	8230	70.0%
Missing	59		8		1		67	
Donor parity	9957		1794	0.1666	698	<0.0001	11751	
M	6985	70.2%	1245	69.4%	524	75.1%	8230	70.0%
F Nonparous	1886	18.9%	370	20.6%	137	19.6%	2256	19.2%
F Parous	1086	10.9%	179	10.0%	37	5.3%	1265	10.8%
Missing	59		8		1		67	
Sex match	9957		1794	0.8539	698	0.7195	11751	
Yes	5751	57.8%	1032	57.5%	408	58.5%	6783	57.7%
Missing	59		8		1		67	
CMV match	9962		1786	0.7653	691	0.4890	11748	
Yes	5560	55.8%	990	55.4%	395	57.2%	6550	55.8%
Missing	54		16		8		70	
DPB1 match	8526		1535	0.4652	603	0.3261	10061	
M/P	6430	75.4%	1171	76.3%	444	73.6%	7601	75.5%
Missing	1490		267		96		1757	
DQB1 match	9810		1773	0.6492	689	0.1282	11583	
Yes	9377	95.6%	1699	95.8%	667	96.8%	11076	95.6%
Missing	206		29		10		235	

CMV: cytomegalovirus, F: female, M: male,
M/P: either a match or a permissive mismatch [Zino et al., 2004]

Table 3: Disease and transplant characteristics. Training and validation sets are mutually exclusive while search archive is a subset of validation. Within the total rows, we present Pearson's Chi-squared test p-values for the comparisons between training with validation and training with search archive: missing values excluded. **Bold** variables are included in the model.

	Training set		Validation set		Search archive		Overall total	
Disease	10016		1802	0.0380	699	0.1416	11818	
ALL	1290	12.9%	251	13.9%	102	14.6%	1541	13.0%
AML	3956	39.5%	746	41.4%	290	41.5%	4702	39.8%
MDS	1988	19.8%	362	20.1%	139	19.9%	2350	19.9%
Other	2782	27.8%	443	24.6%	168	24.0%	3225	27.3%
ALL/AML/MDS status	6947		1306	0.9271	505	0.0398	8253	
Early	4159	59.9%	775	59.3%	279	55.2%	4934	59.8%
Intermediate	1360	19.6%	261	20.0%	99	19.6%	1621	19.6%
Advanced	1428	20.6%	270	20.7%	127	25.1%	1698	20.6%
Missing	287		53		26		340	
Graft type	10016		1802	0.3259	699	0.8784	11818	
Bone marrow	2239	22.4%	384	21.3%	158	22.6%	2623	22.2%
Peripheral blood	7777	77.6%	1418	78.7%	541	77.4%	9195	77.8%
Total body irradiation	9925		1781	0.9647	695	0.3402	11706	
Yes	2397	24.2%	431	24.2%	179	25.8%	2828	24.2%
Missing	91		21		4		112	
Conditioning regimen	10016		1802	0.7367	699	0.4458	11818	
Myeloablative	4974	49.7%	885	49.1%	364	52.1%	5859	49.6%
Non-myeloablative	1122	11.2%	213	11.8%	77	11.0%	1335	11.3%
Reduced intensity	3920	39.1%	704	39.1%	258	36.9%	4624	39.1%
GVHD prophylaxis	10016		1802	0.0676	699	0.0026	11818	
CSA+MMF	430	4.3%	84	4.7%	40	5.7%	514	4.3%
CSA+MTX	356	3.6%	61	3.4%	30	4.3%	417	3.5%
CSA only	65	0.6%	14	0.8%	7	1.0%	79	0.7%
Cyclophosphamide	1130	11.3%	216	12.0%	49	7.0%	1346	11.4%
FK506+MMF	1097	11.0%	209	11.6%	89	12.7%	1306	11.1%
FK506+MTX	5425	54.2%	965	53.6%	377	53.9%	6390	54.1%
FK506 only	1020	10.2%	196	10.9%	82	11.7%	1216	10.3%
Other	493	4.9%	57	3.2%	25	3.6%	550	4.7%
Year of transplant	10016		1802	0.3262	699	<0.0001	11818	
2016	2347	23.4%	419	23.3%	336	48.1%	2766	23.4%
2017	2527	25.2%	438	24.3%	324	46.4%	2965	25.1%
2018	2593	25.9%	450	25.0%	33	4.7%	3043	25.7%
2019	2549	25.4%	495	27.5%	6	0.9%	3044	25.8%

ALL: acute lymphoblastic leukemia, AML: acute myelogenous leukemia, CSA: Ciclosporin A, FK506: tacrolimus, GVHD: graft vs. host disease, MDS: myelodysplastic syndrome, MMF: mycophenolate mofetil, MTX: methotrexate

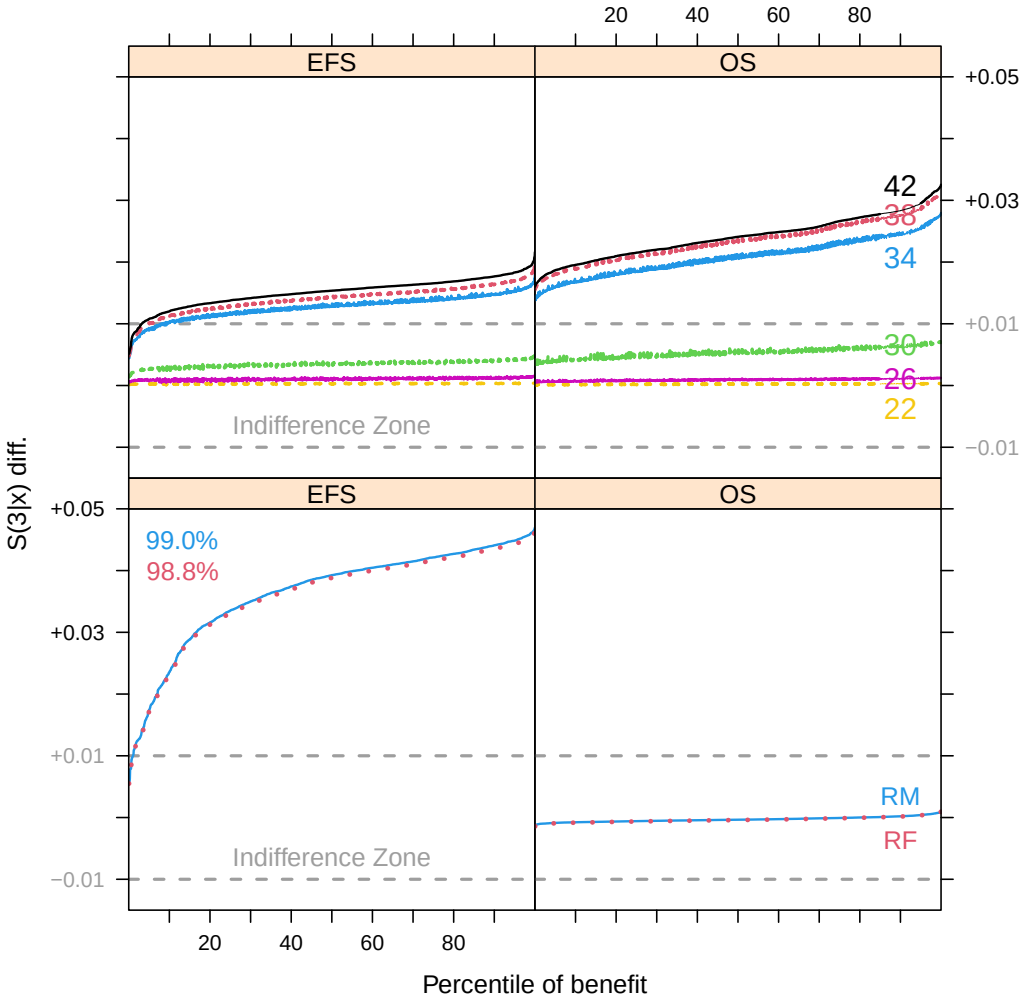

Figure 1: Waterfall plots of EFS and OS differentials based on predictions for the validation set. In the first (second) column, we have EFS (OS) differentials on the vertical axis, with an Indifference Zone in grey, and percentile of benefit on the horizontal axis. In the top row, differentials for an older donor vs. an 18 year-old; donor ages (lines) in ascending sequence: 22 (dashed yellow), 26 (solid magenta), 30 (dashed green), 34 (solid blue), 38 (dashed red) and 42 (solid black). In the bottom row, differentials for a male donor vs. a female; recipient male (female) with a solid blue line (dotted red line): in the left panel, the percentage of those that benefit from a male vs. female donor for recipient males (females) in blue (red).

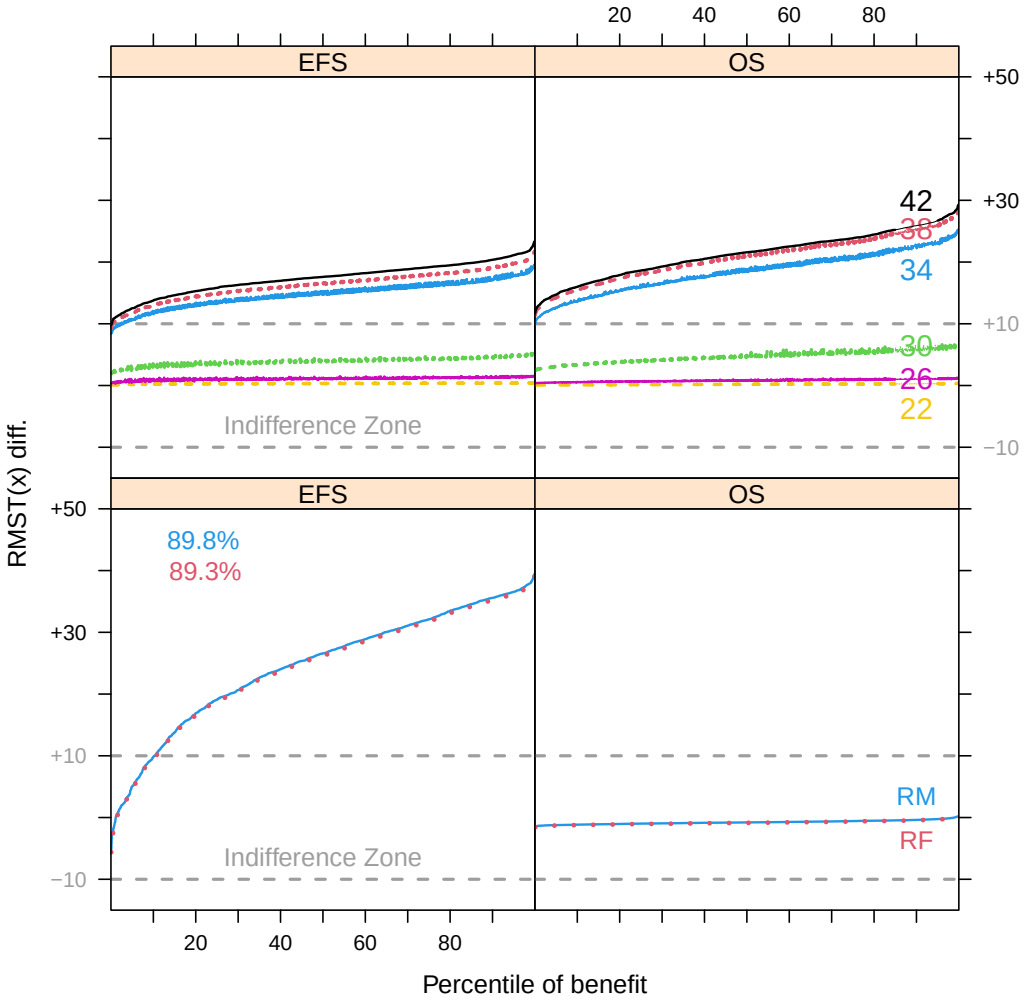

Figure 2: Waterfall plots of EFS and OS differentials based on RMST predictions in days for the validation set. In the first (second) column, we have EFS (OS) RMST differentials on the vertical axis, with an Indifference Zone in grey, and percentile of benefit on the horizontal axis. In the top row, differentials for an older donor vs. an 18 year-old; donor ages (lines) in ascending sequence: 22 (dashed yellow), 26 (solid magenta), 30 (dashed green), 34 (solid blue), 38 (dashed red) and 42 (solid black). In the bottom row, differentials for a male donor vs. a female; recipient male (female) with a solid blue line (dotted red line): in the left panel, the percentage of those that benefit from a male vs. female donor for recipient males (females) in blue (red).

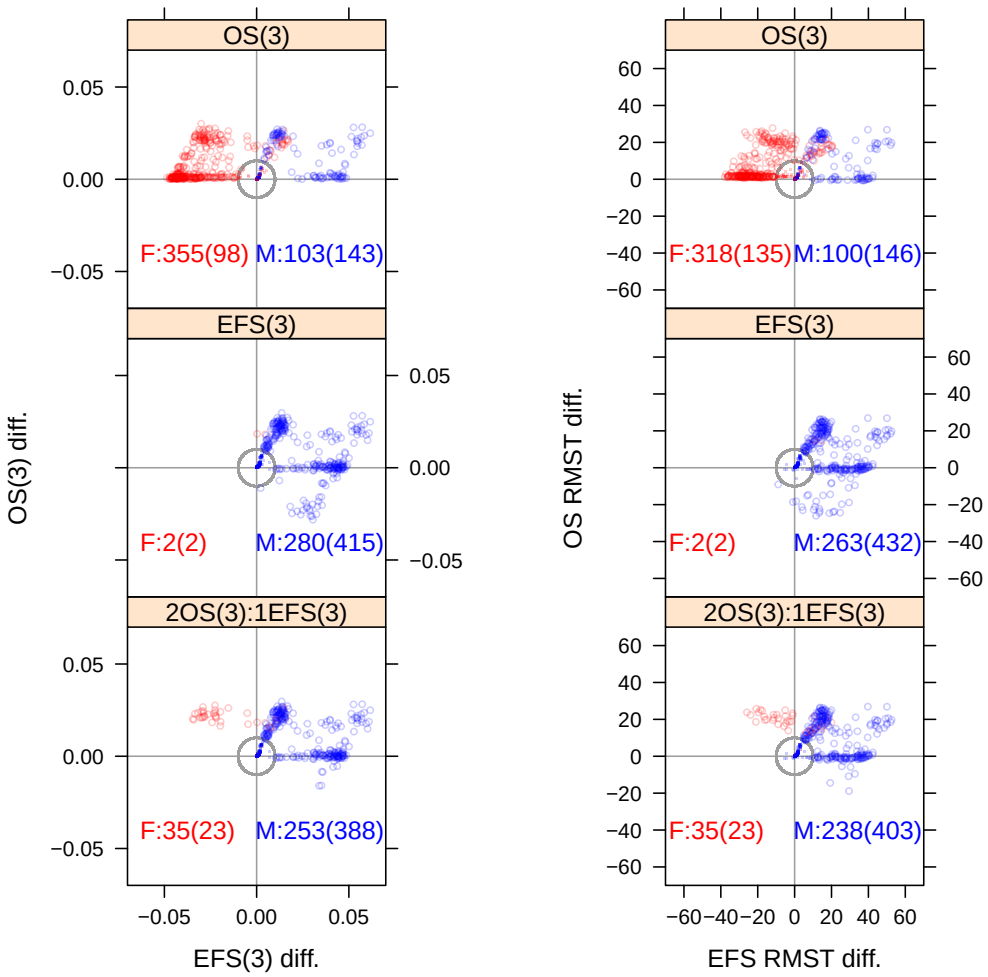

(a) OS/EFS at 3 years

(b) OS/EFS RMST up to 3 years

Figure 3: Optimal donor selection for OS and EFS among search archive recipients. In each row of the figures, optimal is determined by OS (top), EFS (middle) and weighted 2OS:1EFS (bottom) respectively for survival probability differentials at 3 years. On the y-axis (x-axis), we have OS (EFS) differentials of the optimal matching donor vs. the actual donor. At the bottom of each plot, we have a summary of the youngest female (F) donor vs. youngest male (M) chosen: beyond (within) the Indifference Zone is the first summary (second summary in parentheses). Red (blue) circles represent females (males) beyond the Indifference Zone circle boundary (grey line); red (blue) dots are females (males) within the Indifference Zone.

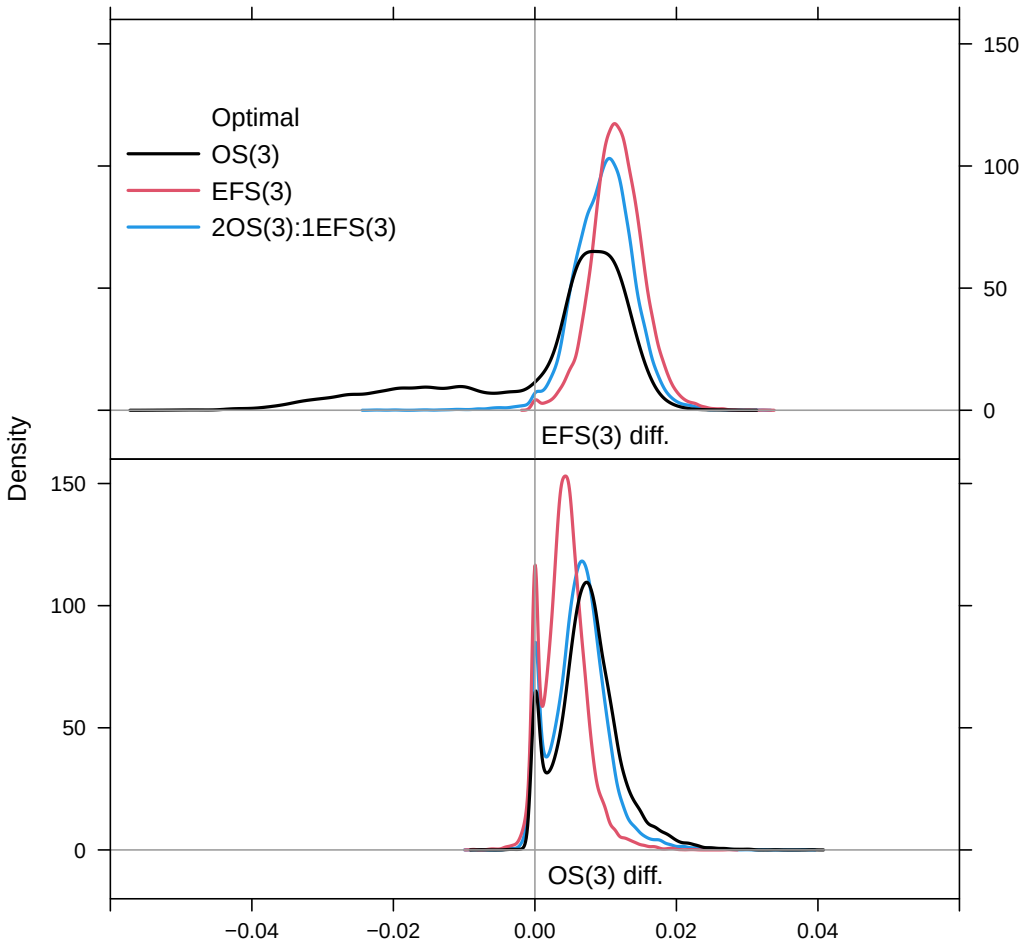

Figure 4: Population-level value function for optimal donor selection survival probability differentials among search archive recipients. The top (bottom) row is for EFS (OS). Three optimal strategy lines are presented for year 3 survival probability differentials: OS (black), EFS (red) and 2OS:1EFS (blue).